High Pressure Thermal Conductivity Measurements of a (Methane + Propane) Mixture with a Transient Hot Wire Apparatus

Sofia K. Mylona[1], Xiaoxian Yang[1], Thomas J. Hughes[1,2], Aaron C. White[1], Luke McElroy[1,3], Dongchan Kim[1], Saif Al Ghafri[1], Paul L. Stanwix[1], Young Hoon Sohn[4], Yutaek Seo[4], Eric F. May[1*]

[1]*Fluid Science & Resources Division, School of Engineering, The University of Western Australia, Perth, Australia*

[2]*Department of Civil Engineering, Monash University, Clayton, VIC 3800, Australia*

[3]*WA School of Mines: Minerals, Energy and Chemical Engineering, Curtin University, Perth, Australia*

[4]*Department of Naval Architecture and Ocean Engineering, Research Institute of Marine Systems Engineering, Seoul, Republic of Korea*

to be submitted to *J. Chem. Eng. Data* (2020)

Abstract

The transient hot-wire (THW) technique is an absolute technique for measuring the thermal conductivity of fluids. In this work, a THW apparatus was developed for measurements over the temperature range from (193 to 424) K at pressures to 34 MPa. The apparatus was commissioned with the measurements of pure argon, methane and propane along several isotherms at pressures to 33 MPa. The measured values agreed with those calculated with the reference equations within the uncertainty of the equations. Thermal conductivity measurements of a binary mixture (0.9514 methane + 0.0486 propane) were then carried out in the temperature range from (195 to 424) K at pressures to 31 MPa in the single phase and near the bubble point curve. The relative combined expanded uncertainty (k = 2) for these single-phase and bubble-point mixture measurements was estimated as 2.0 % and 5.0 %, respectively. The relative deviations of these measured values from those calculated with the extended corresponding states model implemented in the software package REFPROP 10.0 were within 4.4 % and 8.0 %, respectively.

[*]Corresponding author. *Email address:* eric.may@uwa.edu.au.

1. Introduction

Accurate knowledge of the thermal conductivity of fluids plays an important role in many industries especially those involving refrigerators, natural gas, and petroleum. For instance, the design margin for a heat exchanger can be significantly reduced if accurate values of thermal conductivity of the working fluid are available. Values of thermal conductivity are generally calculated with equations implemented in engineering software that are anchored to and correlated with relevant experimental data. In this work, an apparatus based on the transient hot-wire (THW) technique was developed to enable measurements of thermal conductivity for fluids over extended temperature and pressure ranges.

The THW technique is an absolute and commonly used (Perkins et al[1, 2], Assael et al[3, 4], Wu et al.[5, 6], etc) technique for measuring the thermal conductivity of fluids. An early example of its use was by Stalhane and Pyk[7] in 1931 who measured the thermal conductivity of solids and powders. The technique took a leap forward in 1971 due to Haarman[8] who used two wires of different lengths for the first time and introduced the electronic Wheatstone bridge that is a common feature of the modern transient methods. In 1976, Healy et al.[9] developed the theory of the THW described by an ideal solution with appropriate corrections to address various effects. The work of Stalhane and Pyk[7], Haarman[8] and Healy et al.[9] laid a solid foundation for the modern THW technique. A detailed historical development of the technique has been detailed by Wakeham et al.[10] and by Assael et al.[11].

A design based on the THW apparatus of Perkins et al[12, 13] for gas measurements was adapted in this work to enable measurements of gas, liquid, and supercritical fluids in the temperature T range from (193 to 424) K and at pressures p to 34 MPa. The apparatus was commissioned with the measurements of pure argon, methane and propane, and then a binary system (0.9514 methane + 0.0486 propane) was investigated for the purpose of improving the data situation for mixtures. The density[14] and viscosity[15, 16] of this binary mixture had been investigated previously at similar conditions via measurements conducted by our group. Only a few experimental thermal conductivity data can be found in the literature[17, 18] for this binary system and most of them were measured at atmosphere pressure. Here, measurements for this binary mixture were carried out in the temperature range from (195 to 424) K at pressures to 31 MPa in the liquid phase or in the supercritical region, as well as in the vicinity of the fluid's bubble point curve.

In the remainder of the paper, we first summarise the theory for the THW technique and the working equations adopted in this work (Section 2). The experimental setup is explained in detail together with the materials used and procedures followed in Section 3. A detailed uncertainty analysis is presented in Section 4. In Section 5, the measurement results for the pure fluids and the binary mixture (0.9514 methane + 0.0486 propane) are presented and

compared to the predictions of models for thermal conductivity. Finally, Section 6 presents brief conclusions.

2. Working equations

2.1. The ideal equation

With the THW technique, the thermal conductivity of a fluid λ is determined by monitoring the rate at which the temperature of a thin wire immersed in the fluid increases with time t after a step change of voltage is applied to the wire. The temperature response is first considered in the context of an ideal model, in which a thin vertical wire of infinite length l, zero heat capacity $c_{p,\mathrm{w}}$ and infinite thermal conductivity λ_{w} is immersed in a fluid of infinite extent with thermal diffusivity κ, thermal conductivity λ and density ρ. The system is initially at thermodynamic equilibrium with temperature T_0. For this ideal system, when a constant heat flux per unit length q is generated in the thin wire, Fourier's law of thermal conduction is applied under the assumptions that the wire radius r ($\leq$ 10 μm) and the time t ($\leq$ 1 s) are small. The temperature increase ΔT of the wire as a function of time is then given by (see Healy et al.[9] for a detailed derivation):

$$\Delta T(t) = \frac{q}{4 \cdot \pi \cdot \lambda} \cdot \ln\left(\frac{4 \cdot \kappa \cdot t}{r^2 \cdot e^{\gamma}}\right) \tag{1}$$

where γ = 0.5772156649… is the Euler constant.

2.2. Corrections to theory

Equation (1) was derived for an ideal system. However, in any actual experimental setup many of the ideal model's assumptions are not valid: for example, the wire is not infinite in length, the heat capacity of the wire is not zero, and the fluid is bounded in extent. All these factors result in deviations between the observed temperature increase ΔT_{exp} and the ideal one ΔT. The deviation resulting from the finite length of the wire can be significantly reduced by conducting a differential measurement using two wires with different lengths and a Wheatstone bridge; this will be discussed in more detail in section 2.3. For the other corrections, Healy et al.[9] derived a series of equations to estimate their magnitude. The overall correction equation is:

$$\Delta T = \Delta T_{\mathrm{exp}} + \sum_i \delta T_i \tag{2}$$

where δT_i denotes the deviation of the temperature increase due to the correction i. In this work, as suggested by Healy et al.[9], two main corrections were considered.

The first correction is for the finite heat capacity of the wire, which is given by

$$\delta T_1 = r^2 \cdot \frac{\left[\rho_{\mathrm{w}} \cdot c_{p,\mathrm{w}} - \rho \cdot c_p\right]}{2 \cdot \lambda \cdot t} \cdot \Delta T_{\mathrm{exp}} \tag{3}$$

where ρ_{w} is the density of the wire. This correction requires an estimate of the fluid's thermal conductivity λ. An initial value can be obtained from a reference equation for the fluid and then an iterative procedure can be used in the solution of equations (1) - (3) for λ.

Second, the fluid is contained in a measuring cell, usually a cylinder, with finite boundaries. The heat flux through the fluid ultimately raises the temperature of the wall of the cylinder, resulting in a temperature increase of the wire that is less than the ideal value. The finite outer boundary correction is given by

$$\delta T_2 = \frac{q}{4 \cdot \pi \cdot \lambda} \cdot \left[\ln\left(\frac{4 \cdot \kappa \cdot t}{b^2 \cdot e^{\gamma}}\right) + \sum_{\nu=1}^{N} e^{-\frac{g_\nu^2 \cdot \kappa \cdot t}{b^2}} \cdot \left[\pi \cdot Y_0(g_\nu)\right]^2 \right] \tag{4}$$

where b is the diameter of the measuring cell; Y_0 is the second kind Bessel function of first order and g_ν represents the consecutive roots of the first kind Bessel function $J_0(g_\nu) = 0$. In practice the infinite series is evaluated by truncating the summation: in this work, N was set equal to 17 at which point the change in the sum's value was less than 0.001 %. This correction is applicable over the range of $4/\exp(\gamma) < b^2/(\kappa t) < 5.78$.

In principle, several other idealised assumptions used in the derivation of eq (1) need to be corrected for, such as the finite thermal conductivity of the wire, convection[9] in the fluid, the Knudsen effect[9], radiative heat transfer[19], the finite diameter of the wire[20] and compression work[9, 19]. However, the impact of these corrections can, in general, be reduced to a negligible level with a careful design of the experimental setup[19].

In reporting the experimental (T, p, λ) values measured for a fluid, the temperature T is necessarily higher than the equilibrium temperature T_0 because of the heat flux generated by in wire. By assuming a linear increase in the thermal conductivity with temperature of the fluid over the very short experimental time, the reported T can be related to T_0 by

$$T = T_0 + \left(\Delta T\left(t_{\mathrm{s}}\right) + \Delta T\left(t_{\mathrm{e}}\right)\right)/2 \tag{5}$$

where t_{s} and t_{e} are the start and end times of the data selected for analysis. The choice of t_{s} and t_{e} affects the reported result. In this work, t_{e} was set equal to 1 s, and for each measurement, t_{s} was determined by evaluating the linearity of each ($\Delta T(t)$, $\ln(t)$) dataset with t_{s} in the range (0.02 to 0.36) s. The dataset with the highest linearity as quantified by its R^2 value was used to determine the optimal value of t_{s} for the calculation of λ; for all of the data reported here, $R^2 \geq 0.9990$).

2.3. The two-wire technique

The necessity of using a wire of finite length means that end effects cannot be ignored[20]. Kestin and Wakeham[20] utilized a differential method that uses two wires and a Wheatstone bridge to significantly reduce the magnitude of the end effects. By using two wires made of the same material and diameter but with different lengths and applying the same current to both wires, the deviations from ideality due to each wire's end effects are almost the same. To correct for any end effects, a Wheatstone bridge containing each wire within one of its arms is constructed to measure the differential change in resistance associated with each wire's temperature increase. This differential resistance change is interpreted in terms of the temperature rise of a hypothetical working wire, which can in turn be related to the temperature rise of the long wire in the absence of end effects.

A schematic diagram of the Wheatstone bridge arrangement used is presented in Figure 1. The long and short wires with resistances R_L and R_S and lengths l_L and l_S, respectively, are placed in the adjacent arms of the bridge circuit. A known standard resistor, $R_{std} \approx 10\ \Omega$, is placed in the same bridge arm as the long wire to enable quantification of the current that passes through each wire (which are in series). Four variable resistors R_1, R_2, R_3 and R_4 are located in each arm of the bridge to allow it to be balanced. For each measurement the values of R_3 and R_4 are kept constant while prior to triggering the heating current R_2 is adjusted to $R_2 \approx R_L+R_{std}+R_1-R_S$ so that the bridge voltage $V_{bridge} \approx 0$.

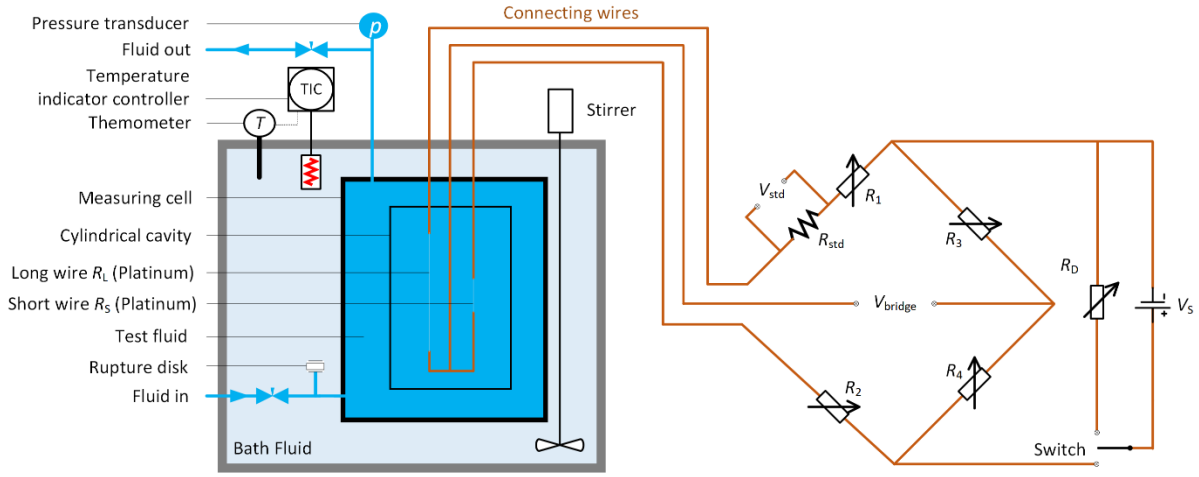

Figure 1. Schematic diagram of the differential THW measurement system showing pressure vessel, thermostat and the Wheatstone bridge.

When a step change in voltage is applied to the Wheatstone bridge for a short period of time, the resistance change $\Delta R_W(t)$ of the working wire at time t can be calculated by:

$$\Delta R_{\mathrm{w}}(t) = 2 \cdot \frac{V_{\mathrm{bridge}}(t)}{V_{\mathrm{std}}(t) / R_{\mathrm{std}}} \tag{6}$$

where $V_{\mathrm{std}}(t)$ is the voltage measured across the standard resistance. The temperature increase of the working wire $\Delta T_{\mathrm{W}}(t)$ can be calculated (see Supporting information A for a detailed derivation) with:

$$\Delta T_{\mathrm{W}}(t) = \frac{-\left[2 \cdot b_{\mathrm{W}} \cdot (T_0 - T_{\mathrm{ref}}) + a_{\mathrm{W}}\right] + \sqrt{\left[2 \cdot b_{\mathrm{W}} \cdot (T_0 - T_{\mathrm{ref}}) + a_{\mathrm{W}}\right]^2 - 4 \cdot b_{\mathrm{W}} \cdot \frac{\Delta R_{\mathrm{W}}(t)}{R_{\mathrm{W}}(T_{\mathrm{ref}})}}}{2 \cdot b_{\mathrm{W}}} \tag{7}$$

where T_{ref} = 273.15 K is a reference temperature, and $\Delta R_{\mathrm{W}}(T_{\mathrm{ref}})$, a_{W} and b_{W} are the parameters for the resistance of the working wire as a function of temperature determined by calibration. According to Kestin and Wakeham[20], the temperature increase in the long wire $\Delta T_{\mathrm{L}}(t)$ can then be calculated by:

$$\Delta T_{\mathrm{L}}(t) = \Delta T_{\mathrm{w}}(t) / (1 + \varepsilon_5) \tag{8}$$

and the heat flux per unit length generated in the long wire q_{L} can be calculated by:

$$q_{\mathrm{L}} = \frac{q_0}{(1 - \varepsilon_1)^2 \cdot (1 + \varepsilon_2)} \tag{9}$$

The equations used to calculate ε_1, ε_2, ε_5, and q_0 from the resistances in the measurement circuit, the source voltage V_S and the wire lengths were derived by Kestin and Wakeham[20] and are summarized in Supporting information B and C.

In summary, T_0, p, $V_{\mathrm{bridge}}(t)$, $V_{\mathrm{std}}(t)$, R_2 and V_{S} are measured values and $\Delta T_{\mathrm{L}}(t)$ is calculated according to Eqs. (6), (7) and (8). Then $\Delta T_{\mathrm{exp}} = \Delta T_{\mathrm{L}}(t)$ is corrected using Eq. (2) to determine the temperature increase of an ideal wire, $\Delta T(t)$. The data set ($\Delta T(t)$, ln(t)) are linearly regressed to Eq. (1) to obtain the slope k_{L} from which the fluid's thermal conductivity can be determined by

$$\lambda = \frac{q_{\mathrm{L}}}{4 \cdot \pi \cdot k_{\mathrm{L}}} \tag{10}$$

with q_{L} calculated by Eq. (9).

3. Experimental

3.1. The measurement system

A schematic diagram of the experimental setup is also illustrated in Figure 1. Two wires, made of platinum (Nilaco, Japan) with diameters approximately 10 μm, were spotted welded to Kapton insulated copper wires, held vertical, and slightly tensioned at both ends within a

cylindrical cavity with a diameter of 9.5 mm. The wires were annealed in situ by several cycles of heating and cooling between the temperatures (273 and 433) K. In the last cycle, the resistances of the wires at each designated temperature changed within 0.01 % from those of the previous cycle, and these values were used for the calibration of the resistances of the wires in Eq. (7). After that, the lengths of the long and short wires were measured with a cathetometer at $T \approx 293.15$ K to be (0.1524 and 0.0459) m, respectively.

The cylindrical cavity was fixed within a high-pressure measuring cell (Confined Gasket Closure Reactor, GC-1, High Pressure Equipment, USA) with operating temperature and pressure limits of 700 K and 83 MPa, respectively. The inlet of the measuring cell was connected to a rupture disk with a set burst pressure of 42 MPa and also to a syringe pump (260D, Teledyne ISCO, USA). The syringe pump was used to control the pressure of the fluids inside the measuring cell. The outlet of the measuring cell was connected to a pressure transducer (Pi642M12-400barg, OMNI, UK) with a relative uncertainty of 0.1 % of full scale 40 MPa. The measuring cell together with the rupture disk were located in a thermostated bath. The bath fluid was silicone oil for experiments conducted at temperatures higher than 298 K, and ethanol for those conducted at lower temperatures. The temperature of the bath fluid was controlled with a stability better than ± 0.01 K using a temperature sensor, a resistive heater and, at lower temperatures, a mixture of ethanol and dry ice. The temperature of the bath fluid was measured by a platinum resistance thermometer (PT100, Correge, France) and was taken to be the same as the temperature of the fluid inside the pressure vessel.

The two platinum wires were connected to a Wheatstone bridge located outside the measuring cell. The standard resistor in the bridge was provided by TE Connectivity, USA, and the variable resistors R_1, R_2, R_3 and R_4 were formed using decade resistance boxes (RBB6-B, Cropico, UK) with six decades and a resolution of 0.001 Ω. The extent of imbalance, V_{bridge}, was measured using a multimeter (34410A, Agilent, USA). A power supply (E3648A, Agilent, USA) was connected to the bridge and a dummy variable resistor R_D in parallel. The dummy resistor had a resistance equal to the total resistance of the Wheatstone bridge to ensure that a more ideal step impulse would be applied to the wires when power was switched the bridge.

3.2. Materials and Procedure

The pure gases were all provided by Coregas, Australia and were used as received from the supplier without further gas analysis or purification. Detailed information of the sample gases is listed in Table 1. The binary mixture (0.9514 methane + 0.0486 propane) was prepared gravimetrically in our laboratory. The expanded uncertainty ($k = 2$) in the mole fraction of the mixture was estimated to be 0.0003 mole fraction.

Table 1 Gas sample information

Chemical name	CAS Reg. No.	Source	Purity/mole fraction	Purification method
Methane	74-82-8	Coregas	0.99995[a]	none
Argon	7440-37-1	Coregas	0.99999[b]	none
Propane	74-98-6	Coregas	0.9999[c]	none

[a] Impurities (stated by supplier): $x(H_2O) \leq 5\times10^{-6}$, $x(O_2) \leq 4\times10^{-6}$, x(other C_mH_n) $\leq 20\times10^{-6}$, $x(N_2) \leq 20\times10^{-6}$, $x(H_2) \leq 1\times10^{-6}$, where x denotes mole fraction.
[b] Impurities (stated by supplier): $x(H_2O) \leq 1.5\times10^{-6}$, $x(O_2) \leq 1.0\times10^{-6}$, $x(C_mH_n) \leq 0.5\times10^{-6}$, $x(CO_2) \leq 0.5\times10^{-6}$, $x(N_2) \leq 5.0\times10^{-6}$.
[c] The main impurities are the other hydrocarbons.

Prior to each thermal conductivity measurement, the Wheatstone bridge was balanced by providing a low voltage (V_S = 0.05 V) to the bridge (switching the power supply from the dummy resistor to the bridge), and then adjusting the value of resistor R_2 so that the bridge imbalance V_{bridge} became zero. This operation was finished (switching the power supply back to the dummy resistor) within a short period of time (≤ 10 s) to minimise the disturbance to the thermal equilibrium in the pressure vessel. After balancing, at least 1 min was allowed for the system to return to equilibrium state.

The power supply voltage was then adjusted to the desired value for the measurement, typically in the range (2 to 6) V. This voltage range produces an experimental temperature rise of (1 to 2) K which is sufficient to both mitigate the effects of electrical noise (that can afflict low temperature increases) or convection (caused by too large temperature rise). The measurement was started by switching the power supply to the bridge and then stopped automatically after 1 s by switching the power supply back to the dummy resistor. In this one second, 51 values of $V_{bridge}(t)$ and $V_{std}(t)$ were recorded with the same sampling time interval.

4. Uncertainty analysis

Following the "Guide to the Expression of Uncertainty in Measurement"[21], the combined expanded uncertainty of the experimental thermal conductivity $U_C(\lambda)$ was estimated by:

$$U_C(\lambda) = \left[U_{meas}(\lambda)^2 + U_{para}(\lambda)^2 + U_{calc}(\lambda)^2 + U_{comp}(\lambda)^2 \right]^{0.5}. \quad (11)$$

where $U_{meas}(\lambda)$, $U_{para}(\lambda)$, $U_{calc}(\lambda)$ and $U_{comp}(\lambda)$ are uncertainties associated with the measured quantities, parameters, calculations and compositions of the mixture, respectively. Note that unless otherwise stated, all uncertainties in this work are expanded uncertainties (k = 2) with a confidence level of 95 %.

4.1. Uncertainty in the measured quantities

The uncertainty in thermal conductivity attributed to measurements $U_{\mathrm{meas}}(\lambda)$ was determined by

$$U_{\mathrm{meas}}(\lambda)=\left[\sum_i\left(\left(\frac{\partial\lambda}{\partial M_i}\right)_{M_j,j\neq i}\cdot U(M_i)\right)^2\right]^{0.5}, \tag{12}$$

where M_i represents: T, p, V_{std}, V_{bridge}, R_2, and V_{S}. There are not explicit expressions for the partial derivatives, therefore, a sensitivity analysis was conducted to estimate the partial derivatives by:

$$\left(\frac{\partial\lambda}{\partial M_i}\right)_{M_j,j\neq i}=\max\left(\left|\frac{\lambda(M_i+\Delta M_i)-\lambda(M_i)}{\Delta M_i}\right|,\left|\frac{\lambda(M_i-\Delta M_i)-\lambda(M_i)}{\Delta M_i}\right|\right) \tag{13}$$

where ΔM_i is the uncertainty of M_i. The uncertainty in temperature was estimated to be $U(T)$ = 0.10 K, which resulted from the calibration uncertainty of the thermometer (0.03 K), the temperature fluctuations present during a measurement (0.002 K), the temperature gradient throughout the measuring cell (0.07 K), and the uncertainty attributed to the multimeter's resistance measurement (0.06 K). The pressure measurement uncertainty was estimated as $U(p)$ = 40 kPa based on the specification of the transducer's manufacturer (0.1 % of full scale 40 MPa). The uncertainties of V_{std}, V_{bridge}, R_2, and V_{S} were all obtained from the manuals provided by the manufacturers: $U(V_{\mathrm{std}})$ = $U(V_{\mathrm{bridge}})$ = 0.0050 % of reading + 0.0035 % of range (100 mV), $U(V_{\mathrm{S}})/V_{\mathrm{S}}$ = 0.2 %, and $U(R_2)/R_2$= 0.05 %.

4.2. Uncertainty in the parameters

The uncertainty contribution from the parameters $U_{\mathrm{para}}(\lambda)$ used in the data analysis was calculated by:

$$U_{\mathrm{para}}(\lambda)=\left[\sum_i\left(\left(\frac{\partial\lambda}{\partial P_i}\right)_{P_j,j\neq i}\cdot U(P_i)\right)^2\right]^{0.5}, \tag{14}$$

where P_i represents: R_1, R_3, R_4, $R_{\mathrm{L,lead}}$, $R_{\mathrm{S,lead}}$, α_T, r_{cell}, r, ρ, c_p, $\rho_{\mathrm{,wire}}$, $c_{p,\mathrm{wire}}$, R_{std}, R_{L}, R_{S}, R_{W}, l_{L}, and l_{S} (see also the Supporting information for the meanings of these parameters). A sensitivity analysis similar to that of equation (13) was adopted to calculate the partial derivatives. The uncertainties of R_1, R_3, and R_4 were obtained from the manuals provided by the manufacturer. The relative uncertainties of $R_{\mathrm{L,lead}}$, $R_{\mathrm{S,lead}}$, α_T and r_{cell} were roughly estimated as 5.0 %. The value of the wire radius r was determined with the SEM (scan electron microscope) to be (5.0 ± 0.1) μm as the average over a length of wire. The uncertainty of ρ and c_p were obtained from

the GERG-2008 equation of state[22]: $U(\rho)/\rho$ = 0.1 % and $U(c_p)/c_p$ = 2.0 %. The uncertainties of ρ_{wire} and $c_{p,\text{wire}}$ were estimated based on the change of the values from room temperature to the highest investigated temperature, which were $U(\rho_{\text{wire}})/\rho_{\text{wire}}$ = 0.1 % and $U(c_{p,\text{wire}})/\ c_{p,\text{wire}}$ = 2.0 %[23] respectively. The relative uncertainty of R_{std} was estimated as 0.1 % with the variation of the room temperature and the drift of the resistance with time taken into consideration. The uncertainties of R_{L}, R_{S} and R_{W} were obtained from the independent calibration with $U(R_{\text{L}})/R_{\text{L}}$ = 0.1 %, $U(R_{\text{S}})/R_{\text{S}}$ = 0.2 %, and $U(R_{\text{W}})/R_{\text{W}}$ = 0.3 %. The uncertainty of the length of the platinum wires l_{L} and l_{S} over the whole investigated temperature range was estimated to be 0.0002 m.

4.3. Uncertainty in calculations

The value of the thermal conductivity was determined using the model presented in Section 2. The model itself has been simplified and various corrections were applied; the effect of the simplification and corrections were estimated to be $U_{\text{model}}(\lambda)/\lambda$ = 1.0 %, which is in the same order as the repeatability of the measurements. In regressing equation (1), the choice of t_{s} and t_{e} affects the reported result; the effect was estimated as $U_{\text{regress}}(\lambda)/\lambda$ = 0.2 % based on adding and subtracting 5 % of the data used in the regression. At each *T*-*p* state point, measurements were repeated at least twice and at most eight times; the scatter $U_{\text{scatter}}(\lambda)$ should be taken into consideration as well. In summary, the uncertainty in thermal conductivity attributed to the calculation $U_{\text{calc}}(\eta)$ was estimated by:

$$U_{\text{calc}}(\lambda) = \left[U_{\text{model}}(\lambda)^2 + U_{\text{regress}}(\lambda)^2 + U_{\text{scatter}}(\lambda)^2 \right]^{0.5}. \tag{15}$$

4.4. Uncertainty in compositions

As discussed in section 3.2, the uncertainty in composition of the mixture attributed to the mixture preparation was $U_{\text{prepare}}(x)$ = 0.0003 mole fraction. Other uncertainty sources included the impurities introduced to the fluid sample when injected from the syringe pump to the measuring cell, and the potential for inadvertent composition change due to flashing upon the mixture entering the evacuated cell. These effects were summed up to $U_{\text{other}}(x)$ = 0.0010 mole fraction. The uncertainty in thermal conductivity due to the composition variation was estimated using the ECS model implemented in the software REFPROP 10.0[24].

4.5. Uncertainty summary

A budget for the combined uncertainty in the thermal conductivity $U_{\text{C}}(\lambda)$ is summarized in Table 2 with the measurement of the mixture (0.9514 methane + 0.0486 propane) at *T* = 200.79 K and *p* = 13.83 MPa taken as an example condition. The simplification and correction of the model and the scatter of repeated measurements are the dominant contributions. The

value $U_C(\lambda)/\lambda$ was estimated to be 2.0 % for single-phase pure fluid measurements, and 2.0 % and 5.0 % for the single-phase and bubble-point mixture measurements, respectively.

Table 2 Uncertainty budget for the thermal conductivity. The contributions refer to the measurement of (0.9514 methane + 0.0486 propane) at T = 200.79 K and p = 13.83 MPa.[a]

Source	Uncertainty U	Contribution to $U_C(\lambda)/\lambda$
Temperature T	100 mK	0.02 %
Voltage on standard resistor V_{std}	0.02 %	0.02 %
Bridge imbalance V_{bridge} (1.5 mV)	0.3 %	0.30 %
Variable resistor R_2	0.05 %	0.03 %
Power supply V_S	0.1 %	0.20 %
Wire radius r (5.0 μm)	0.1 μm	0.03 %
Heat capacity of the wire $c_{p,wire}$	2.0 %	0.02 %
The standard resistor R_{std}	0.1 %	0.11 %
Resistance of the long wire R_L	0.1 %	0.05 %
Resistance of the short wire R_S	0.2 %	0.15 %
Resistance of the working wire R_W	0.3 %	0.30 %
Length of the long wire l_L (0.1515 m)	0.0002 m	0.19 %
Length of the short wire l_S (0.0466 m)	0.0002 m	0.18 %
Regression	10 % of data	0.20 %
Simplification and correction of the model	1.0 %	1.00 %
Scatter of the repeated measurements	1.1 %	1.10 %
Summary: Combined uncertainty for pure fluids $U_C(\lambda)/\lambda$		1.61 %
Summary: Combined uncertainty for this mixture $U_C(\lambda)/\lambda$		1.61 %

[a] Uncertainty contributions to $U_C(\lambda)$ associated with pressure measurement p, parameters R_1, R_3, R_4, $R_{L,lead}$, $R_{S,lead}$, α_T, r_{cell}, ρ, c_p and $\rho_{,wire}$, and mixture compositions are less than 0.01 %.

5. Results

5.1. Pure fluids

Within the scope of commissioning the experimental setup, thermal conductivity measurements were carried out for argon at T = 312.5 K with pressures up to 31 MPa, for methane at (312.7, 368.0 and 423.6) K up to 33 MPa, and for propane at 373.7 K up to 15 MPa. The measurement locations are shown in pressure-temperature phase diagrams in Figure 2 together with those for available data from the literature. The (T, p, λ) measurements were repeated at least twice at each T-p state and all presented in Figure 3(a) as a function of density, while only the averaged results are listed in Table 3. The densities were calculated with the reference equations of state (argon[25], methane[26], propane[27]) implemented in the software REFPROP 10.0[24].

The relative deviations of the experimental thermal conductivity from values calculated with the reference equations (argon[28], methane[29], propane[30]) implemented in REFPROP 10.0[24] are

illustrated in Figure 3(b). The relative deviations are less than 2.2 % for argon, 1.9 % for methane, and 4.8 % for propane. In the density range above 100 $kg \cdot m^{-3}$ for argon, the agreement is as good as 1.0 %. The isotherms of argon along T = 312.5 K, methane along T = 312.7 K and propane along T = 373.7 K in Figure 3(a) were extrapolated to obtain the thermal conductivity, 0.0180, 0.0352 and 0.0272 $W \cdot m^{-1} \cdot K^{-1}$ respectively, at the zero-density limit; all the three values are smaller than the calculations of the reference equations with relative deviations less than 2.0 %. The reported relative uncertainties of these reference equations in the investigated *T-p* range are 2.0 % for argon[25] and methane[26], and 5.0 % for propane[27]; our measurements are generally within the uncertainty of these equations. Comparisons with selected experimental data from the literature as obtained from NIST TDE database[31] are illustrated in Figure 4. In general, the relative deviations of our experimental values from the reference equations are within the scatter of the literature data.

Table 3 Thermal Conductivity measurements of argon, methane and propane[a].

T/ K	p/ MPa	λ/ $W \cdot m^{-1} \cdot K^{-1}$	T/ K	p/ MPa	λ/ $W \cdot m^{-1} \cdot K^{-1}$	T/ K	p/ MPa	λ/ $W \cdot m^{-1} \cdot K^{-1}$
				Argon				
312.23	31.08	0.0342	312.39	20.37	0.0281	312.84	4.91	0.0201
312.24	27.38	0.0324	312.65	17.17	0.0264	312.79	1.95	0.0188
312.20	25.85	0.0314	312.58	13.79	0.0246	312.26	1.08	0.0184
312.13	24.16	0.0303	312.75	10.32	0.0229			
				Methane				
423.90	33.21	0.0772	367.49	27.93	0.0694	312.07	24.18	0.0665
423.59	30.34	0.0750	368.16	26.28	0.0672	311.90	20.69	0.0615
423.36	28.81	0.0738	367.83	24.64	0.0657	312.24	17.27	0.0555
423.49	26.97	0.0724	367.78	21.11	0.0618	312.26	13.70	0.0507
423.51	23.54	0.0685	368.08	17.65	0.0594	312.42	10.28	0.0459
423.43	20.24	0.0665	368.26	14.23	0.0560	312.43	6.15	0.0412
423.69	16.49	0.0631	368.20	10.84	0.0525	311.97	4.57	0.0393
423.78	13.22	0.0615	368.87	5.35	0.0484	312.29	1.70	0.0364
367.41	31.72	0.0733	312.23	25.79	0.0685	312.76	1.09	0.0362
				Propane				
373.57	14.95	0.0836	373.69	8.57	0.0767	374.30	1.87	0.0302
373.58	12.22	0.0800	373.88	3.62	0.0347			
373.51	10.06	0.0771	373.59	3.03	0.0313			

[a] The expanded uncertainties (k = 2) of the measurements are 0.10 K for temperature T, 0.04 MPa for pressure p, and 2.0 % for thermal conductivity λ.

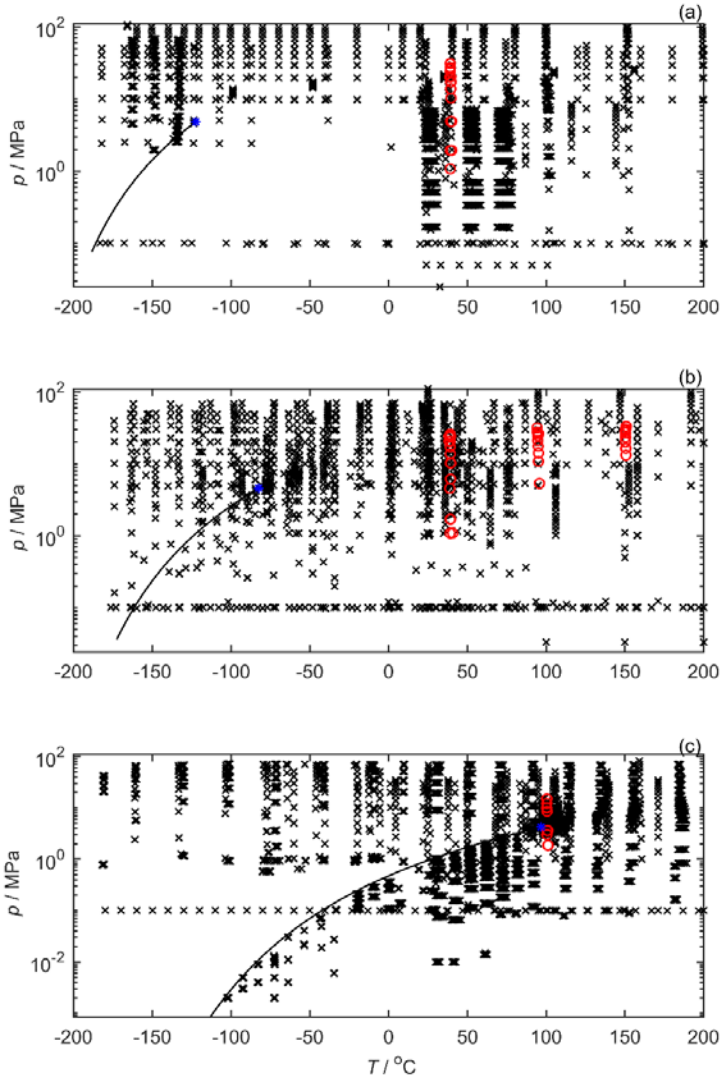

Figure 2. Available experimental (T, p, λ) data from literature (×) and the data measured in this work (○). The solid curves are the vapor-liquid phase boundaries calculated with REFPROP 10.0[24].✳, critical point. Data from the literature were obtained from the NIST TDE database[31]. (a) Argon; (b) Methane; (c) Propane.

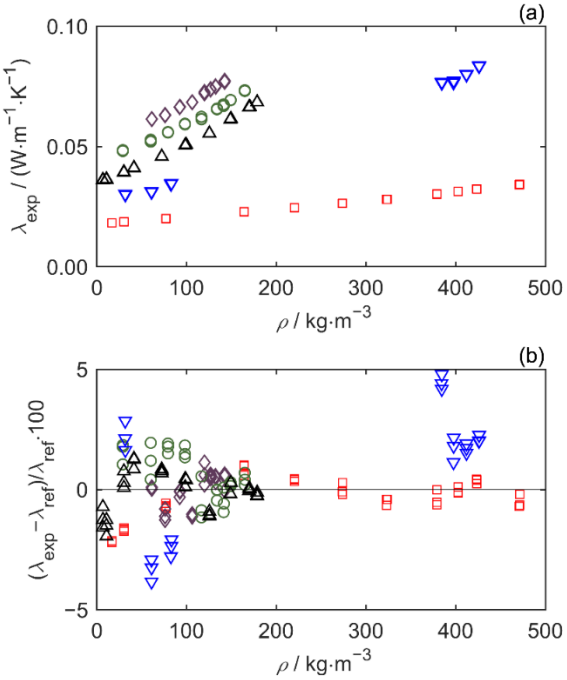

Figure 3 Thermal conductivity of argon, methane and propane. Symbols: □, argon at T = 312.5 K; ◇, methane at T = 423.6 K; ○, methane at T = 368.0 K; △, methane at T = 312.7 K; ▽ propane at T = 373.7 K. (a) Experimental thermal conductivity λ_{exp} as a function of density ρ. (b) Relative deviations of the experimental thermal conductivity λ_{exp} from values λ_{ref} calculated using the reference equations for each fluid (argon[28], methane[29] and propane[30]).

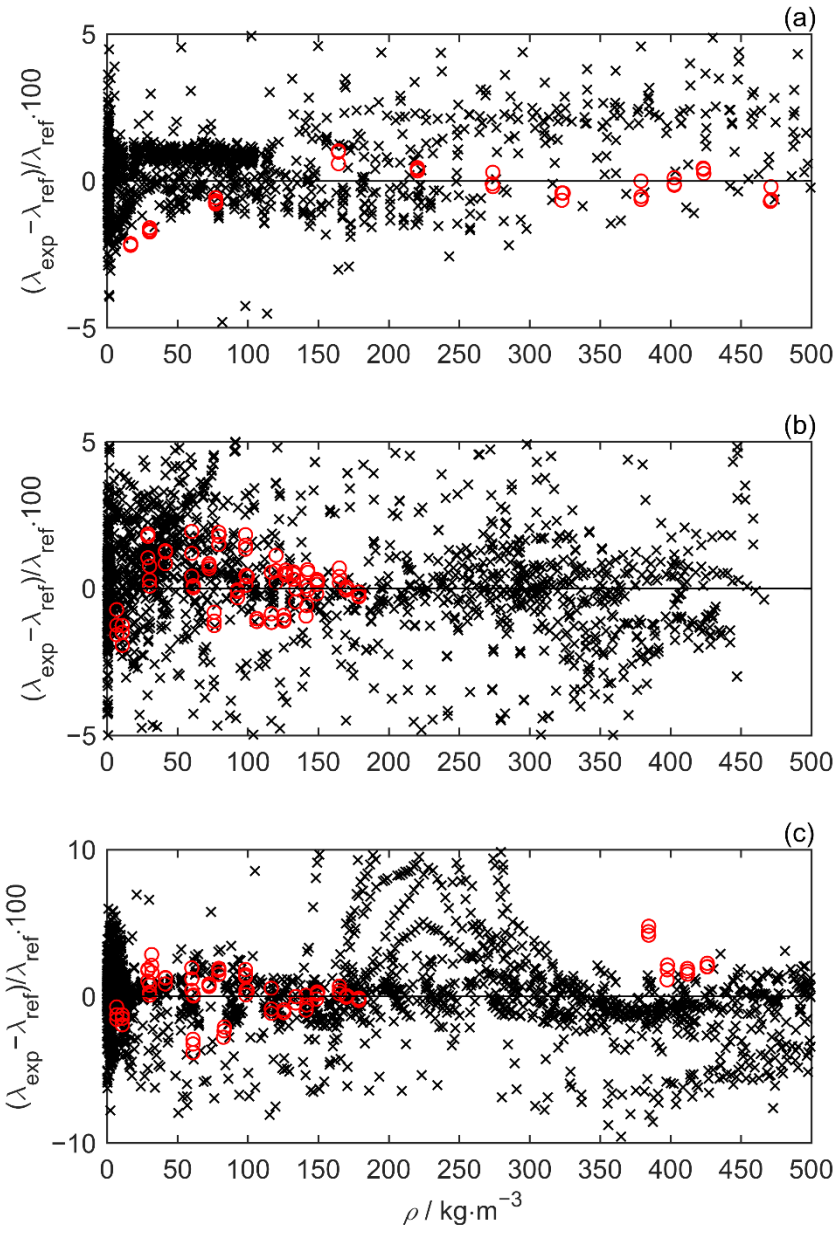

Figure 4 Relative deviations of the experimental thermal conductivity λ_{exp} from values λ_{ref} calculated with each fluid's reference equation (argon[28], methane[29] and propane[30]). ○, data measured in this work; × data from the literature as obtained from the NIST TDE database[31]. (a) Argon; (b) Methane; (c) Propane.

5.2. Binary mixture: 0.9514 methane + 0.0486 propane

Thermal conductivity measurements for the binary mixture (0.9514 methane + 0.0486 propane) were carried out along eight isotherms from (201.4 to 423.6) K at pressures up to 32 MPa in the liquid phase or supercritical region. The experimental temperature increase of the wire ΔT as a function of time t, and the relative deviations from the fit to Eq. (1) *vs* ln(t) are shown in

Figure 5 for the exemplar measurement at T = 200.79 K and p = 13.83 MPa. The measured ΔT values deviate by less than 0.05% from the linear fit to ln(t), indicating correct operation of the THW sensor for this mixture.

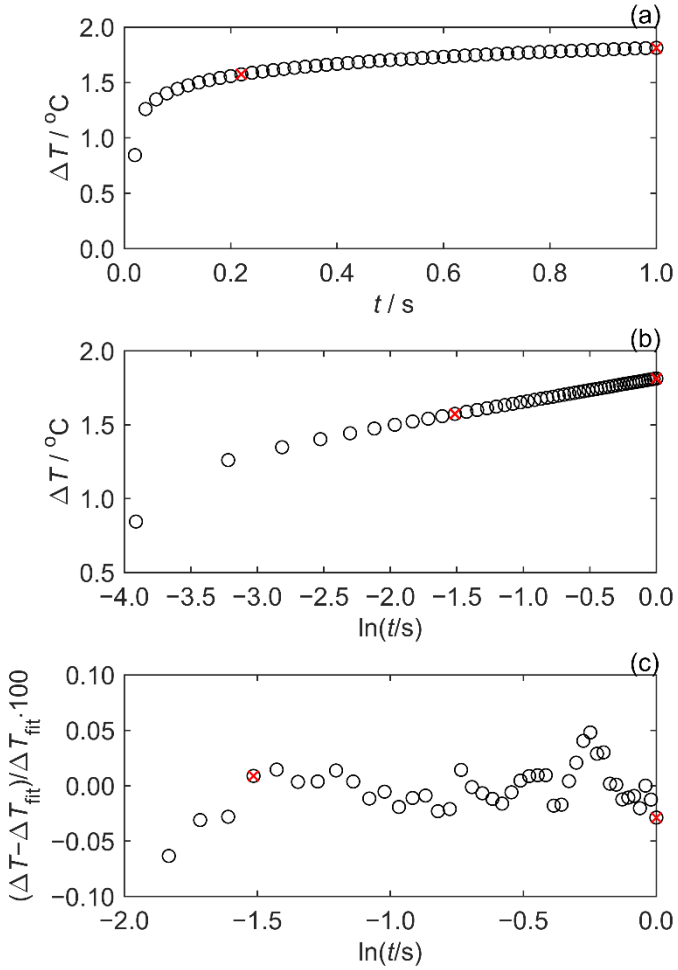

Figure 5 The experimental temperature increase of the wire ΔT as a function of time t (a) and ln(t) (b), respectively, for the binary mixture (0.9514 methane + 0.0486 propane) measurement at T = 200.79 K and p = 13.83 MPa. (c) Relative deviations of ΔT from the fit ΔT_{fit} to Eq. (1) *vs* ln(t). ○, measured points; × indicating the start and end times for the fit.

The conditions at which the thermal conductivity data were measured are illustrated in a pressure-temperature phase diagram shown in Figure 6(a). The experimental (T, p, λ) data are listed in Table 4, and the experimental thermal conductivity is shown as a function of density in Figure 6(b). Mixture densities were calculated using the GERG-2008 equation of state[22] as implemented in REFPROP 10.0[24]. The relative deviations of the experimental thermal conductivity data from values calculated with the extended corresponding states (ECS) model[32] as implemented in REFPROP 10.0[24] and with the SUPERTRAPP model[33] as implemented in MultiFlash[34] are from (−1.5 to 4.4) % and from (−6.6 to −3.3) %, respectively, as illustrated in

Figure 6(c). In general, the ECS predictions are lower than the experimental values while the SUPERTRAPP predictions are higher.

Often, liquids in industrial heat exchangers are at their bubble point and knowledge of the fluid's thermal conductivity at this condition is useful for reliable estimates of heat transfer. However, direct measurements at this saturation condition are difficult, particularly for mixtures given the risk of inadvertent changes in composition. To estimate the thermal conductivity of the binary system at its bubble point, several measurements of the single-phase liquid were measured along isothermal pathways with decreasing pressure steps until the fluid was approximately 1.0 MPa above the bubble point predicted using the GERG-2008 equation[22]. Then the GERG-2008 equation[22] was also used to calculate the single-phase densities at which the thermal conductivity data were obtained. The resulting (ρ, λ) data set was regressed linearly and the best fit function was used to estimate the liquid's thermal conductivity at the bubble-point density ρ_{bubble}. The experimental (T, p, λ) measured data along isotherms $T \approx$ (195.7, 201.4 and 209.3) K are listed in Table 5 together with the extrapolated value of thermal conductivity at the corresponding bubble point: the reported bubble point temperature is the average of the single phase temperatures measured along the isotherm. These measurements are also illustrated in a λ *vs.* ($\rho - \rho_{\text{bubble}}$) plot in Figure 6(d). The relative combined expanded uncertainty (k = 2) in thermal conductivity measurements at the bubble points was estimated to be 5.0 %, based on the increased statistical uncertainty associated with the extrapolation to the bubble point condition. The measured thermal conductivity at the bubble points deviate from those predicted by the ECS model by as much as 5.2 % as shown in Table 5.

Table 4 Thermal Conductivity measurements of the binary mixture (0.9514 methane + 0.0486 propane) [a].

T/ K	p/ MPa	λ/ W·m^{-1}·K^{-1}	T/ K	p/ MPa	λ/ W·m^{-1}·K^{-1}	T/ K	p/ MPa	λ/ W·m^{-1}·K^{-1}
200.48	31.13	0.1302	242.55	27.76	0.0963	312.11	25.88	0.0704
200.49	26.85	0.1245	242.57	25.83	0.0930	312.19	24.13	0.0686
200.50	25.15	0.1225	242.56	24.11	0.0902	312.25	20.86	0.0634
200.41	23.45	0.1193	242.46	20.85	0.0839	367.83	31.53	0.0739
201.29	24.16	0.1188	242.51	17.87	0.0790	367.80	28.12	0.0707
202.15	20.76	0.1128	256.32	31.02	0.0946	367.77	26.37	0.0683
201.89	17.33	0.1077	256.28	27.58	0.0884	367.84	24.63	0.0667
200.79	13.83	0.1032	256.45	25.85	0.0859	367.98	21.19	0.0629
200.92	10.68	0.0950	256.44	24.11	0.0838	423.56	33.55	0.0781
214.33	14.60	0.0911	256.55	20.70	0.0771	423.73	31.09	0.0769
214.30	10.40	0.0795	312.06	31.46	0.0770	423.64	29.38	0.0752
228.62	20.50	0.0926	312.10	31.48	0.0773	423.75	27.70	0.0737
228.59	17.29	0.0865	312.05	27.60	0.0722	423.66	24.22	0.0705
228.24	13.78	0.0773						

[a] The expanded uncertainties (k = 2) of the measurements are 0.10 K for temperature T, 0.04 MPa for pressure p, 0.0010 mole fraction for composition, and 2.0 % for thermal conductivity λ.

Table 5 Thermal conductivity measurements near and extrapolated (bold) to three bubble points of the binary mixture (0.9514 methane + 0.0486 propane)[a], together with values estimated using the ECS model implemented in REFPROP 10.0[24].

T/ K	p/ MPa	λ_{exp}/ W·m^{-1}·K^{-1}	λ_{ECS}/ W·m^{-1}·K^{-1}	$100\cdot(\lambda_{exp}-\lambda_{ECS})/\lambda_{ECS}$
208.53	11.53	0.0907	0.0897	1.1
210.45	9.81	0.0869	0.0828	5.0
210.13	8.57	0.0811	0.0789	2.8
209.27[b]	**6.31**	**0.0662**	**0.0698**	**−5.2**
201.62	9.53	0.0933	0.0916	1.8
201.89	7.55	0.0866	0.0852	1.6
202.25	7.05	0.0837	0.0829	1.0
201.94[b]	**5.50**	**0.0748**	**0.0770**	**−2.8**
195.71	9.04	0.0957	0.0969	−1.3
195.55	8.04	0.0929	0.0945	−1.7
195.89	7.04	0.0939	0.0912	3.0
195.57	6.55	0.0945	0.0900	5.0
195.74[b]	**4.75**	**0.0835**	**0.0829**	**0.7**

[a] The expanded uncertainties (k = 2) of the measurements are 0.10 K for temperature T, and 0.04 MPa for pressure p, 0.0010 mole fraction for composition, and 2.0 % and 5.0 % for the thermal conductivity λ in the single phase and at the bubble points, respectively.
[b]At each bubble point, the stated pressure was estimated using REFPROP 10.0[24].

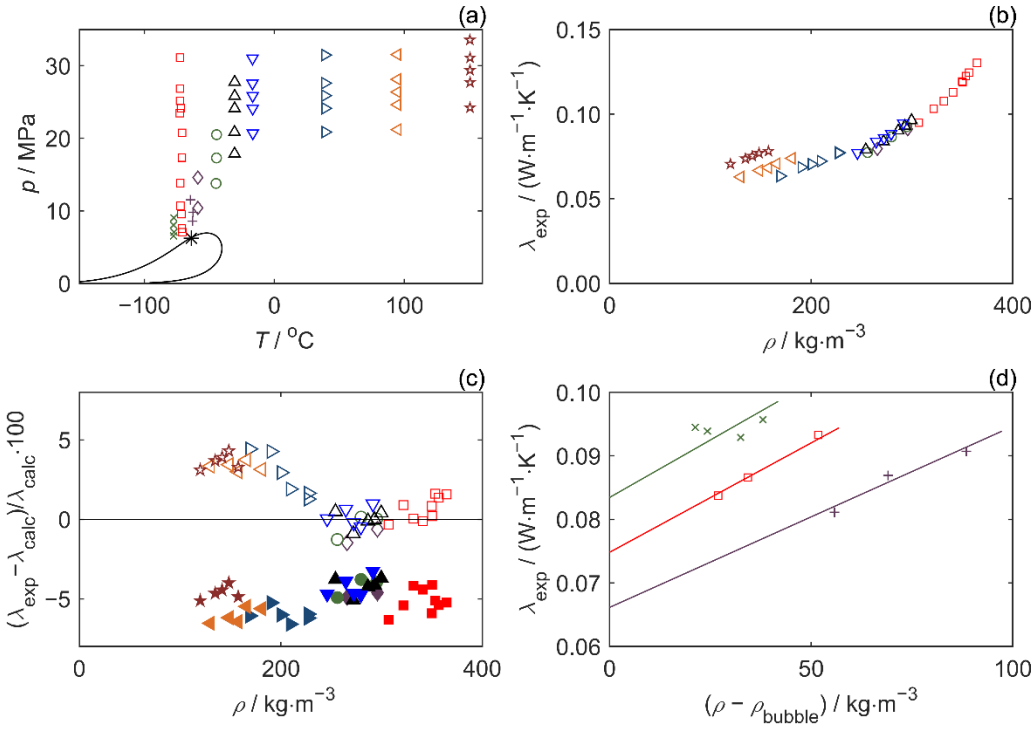

Figure 6 Thermal conductivity measurements of the binary mixture (0.9514 methane + 0.0486 propane). Symbols: ×, T = 195.7 K; □■, T = 201.4 K; +, T = 209.3 K; ◇♦, T = 214.3 K; ○●, T = 228.5 K; △▲, T = 242.5 K; ▽▼, T = 256.4 K; ▷▸, T = 312.1 K; ◁◂, T = 367.8 K; ☆★, $T \approx$ 423.6 K. (a) The pressure-temperature phase diagram and the measurement conditions investigated; the phase boundaries (solid curves) and the critical point (✳) were calculated using the GERG-2008 equation of state[22] as implemented in REFPROP 10.0[24]. (b) Experimental thermal conductivity λ_{exp} as a function of density ρ. (c) Relative deviations of the experimental conductivity λ_{exp} from values λ_{calc} calculated with the ECS model[32] as implemented in REFPROP 10.0[24] (empty symbols) and with the SUPERTRAPP model[33] as implemented in MultiFlash[34] (full symbols). (d) Experimental thermal conductivity λ_{exp} as a function of (ρ−ρ_{bubble}), where ρ_{bubble} is the density at the bubble point predicted by the GERG-2008 equation of state; the straight lines were regressed to the single phase data measured along each isotherm and extrapolated to the bubble point condition (ρ−ρ_{bubble}) = 0 to provide an estimate of the fluid's thermal conductivity at the bubble point.

6. Conclusions

An apparatus utilizing the transient hot-wire technique was developed for measurements of thermal conductivity in fluid mixtures over the temperature range from (193 to 424) K and at pressures to 34 MPa. Thermal conductivity measurements were first carried out on pure argon, methane and propane along several isotherms at pressures to 33 MPa. The combined expanded uncertainty (k = 2) of the thermal conductivity measurement of this apparatus was estimated to be 2.0 % for pure fluids.

Thermal conductivity measurements of a binary mixture (0.9514 methane + 0.0486 propane) were then carried out in the temperature range from (195 to 424) K at pressures up to 31 MPa in the single-phase liquid and supercritical region. Data were also obtained in the vicinity of the fluid's bubble point at three temperatures and extrapolated to estimate the thermal conductivity of the fluid at the saturation condition. The relative combined expanded uncertainty (k = 2) was roughly estimated to be 2.0 % for the single phase mixture measurements and 5.0 % for the experimentally determined values at the bubble-point. The thermal conductivity data were compared with values predicted using the extended corresponding states (ECS) model implemented in the software REFPROP 10.0[24], with the relative deviations having magnitudes less than 4.4 % for the single-phase condition and less than 5.2 % for the bubble-point conditions. The experimental data in the single phase were also compared to values calculated with the SUPERTRAPP model[33] implemented in the software MultiFlash[34] with relative deviations from (−6.6 to −3.3) %. The data measured in this work could be used to adjust the methane-propane binary parameters within the ECS thermal conductivity model: this will be the subject of future work.

Supporting Information Available: [A. Detailed derivation for the relation of the resistance of the working wire and temperature. B. Detail calculation of the temperature increase in the long wire. C. Detail calculation of the heat generation in the long wire.]

Acknowledgments

This work was supported financially by the GPA Midstream Association and the Australian Research Council through LP130101018 and IC150100019.

References

1. Perkins, R. A.; Huber, M. L.; Assael, M. J., Measurements of the thermal conductivity of 1, 1, 1, 3, 3-Pentafluoropropane (R245fa) and correlations for the viscosity and thermal conductivity surfaces. *J. Chem. Eng. Data* **2016,** 61, 3286-3294.
2. Perkins, R. A.; Huber, M. L.; Assael, M. J., Measurement and Correlation of the Thermal Conductivity of trans-1-Chloro-3, 3, 3-trifluoropropene (R1233zd (E)). *J. Chem. Eng. Data* **2017,** 62, 2659-2665.
3. Tertsinidou, G. J.; Tsolakidou, C. M.; Pantzali, M.; Assael, M. J.; Colla, L.; Fedele, L.; Bobbo, S.; Wakeham, W. A., New measurements of the apparent thermal conductivity of nanofluids and investigation of their heat transfer capabilities. *J. Chem. Eng. Data* **2016,** 62, 491-507.
4. Antoniadis, K. D.; Tertsinidou, G. J.; Assael, M. J.; Wakeham, W. A., Necessary Conditions for Accurate, Transient Hot-Wire Measurements of the Apparent Thermal Conductivity of Nanofluids are Seldom Satisfied. *Int. J. Thermophys.* **2016,** 37, 78.

5. Li, X.; Wu, J.; Dang, Q., Thermal Conductivity of Liquid Diethyl Ether, Diisopropyl Ether, and Di-n-butyl Ether from (233 to 373) K at Pressures up to 30 MPa. *J. Chem. Eng. Data* **2010,** 55, 1241-1246.
6. Wang, X.; Qiu, S.; Wu, J., Measurements of the Thermal Conductivity of n-Pentane, Isopentane, 1-Pentene and 1-Pentanol in the Temperature Range from (253 to 373) K at Pressures up to 30 MPa. In *The 12th Asian Thermophysical Properties Conference (ATPC 2019)*, Xi'an, 2019.
7. Stålhane, B.; Pyk, S., Ny metod för bestämning av värmeledningskoefficienter. *Teknisk Tidskrift* **1931,** 61, 389/393.
8. Haarman, J. W., A contribution to the theory of the transient hot-wire method. *Physica* **1971,** 52, 605-619.
9. Healy, J. J.; de Groot, J. J.; Kestin, J., The theory of the transient hot-wire method for measuring thermal conductivity. *Physica B+C* **1976,** 82, 392-408.
10. W.A.Wakeham; Nagashima, A.; (eds.), J. V. S., *Experimental Thermodynamics. Vol. III, Measurement of the Transport Properties of Fluids*. Blackwell Scientific Publications: London, 1991.
11. Assael, M. J.; Antoniadis, K. D.; Wakeham, W. A., Historical Evolution of the Transient Hot-Wire Technique. *Int. J. Thermophys.* **2010,** 31, 1051-1072.
12. Perkins, R.; Roder, H.; de Castro, C. N., A high-temperature transient hot-wire thermal conductivity apparatus for fluids. *J. Res. Natl. Inst. Stand. Technol.* **1991,** 96, 247.
13. Vaughan, K. H. Design of an Apparatus to Measure Thermal Conductivity of Electrically Conducting Fluids. University of Canterbury, New Zealand, 2000.
14. Karimi, A.; Hughes, T. J.; Richter, M.; May, E. F., Density Measurements of Methane + Propane Mixtures at Temperatures between (256 and 422) K and Pressures from (24 to 35) MPa. *J. Chem. Eng. Data* **2016,** 61, 2782-2790.
15. Stanwix, P. L.; Locke, C. R.; Hughes, T. J.; Johns, M. L.; Goodwin, A. R.; Marsh, K. N.; May, E. F., Viscosity of {x CH4+(1–x) C3H8} with x= 0.949 for Temperatures between (200 and 423) K and Pressures between (10 and 31) MPa. *J. Chem. Eng. Data* **2014,** 60, 118-123.
16. Czubinski, F. F.; Al Ghafri, S. Z. S.; Hughes, T. J.; Stanwix, P. L.; May, E. F., Viscosity of a [xCH4+(1− x) C3H8] mixture with x= 0.8888 at temperatures between (203 and 424) K and pressures between (2 and 31) MPa. *Fuel* **2018,** 225, 563-572.
17. Smith, W.; Durbin, L.; Kobayashi, R., Thermal Conductivity of Light Hydrocarbons and Methane-Propane Mixtures at Low Pressures. *J. Chem. Eng. Data* **1960,** 5, 316-321.
18. Cheung, H.; Bromley, L. A.; Wilke, C., Thermal conductivity of gas mixtures. *AlChE J.* **1962,** 8, 221-228.
19. Nieto de Castro, C. A.; Taxis, B.; Roder, H. M.; Wakeham, W. A., Thermal diffusivity measurement by the transient hot-wire technique: A reappraisal. *Int. J. Thermophys.* **1988,** 9, 293-316.
20. Kestin, J.; Wakeham, W. A., A contribution to the theory of the transient hot-wire technique for thermal conductivity measurements. *Physica A: Statistical Mechanics and its Applications* **1978,** 92, 102-116.
21. ISO/IEC Guide 98-3 *Uncertainty of measurement - Part 3: Guide to the expression of uncertainty in measurement (GUM:1995).* International Organization for Standardization, Geneva, 2008.
22. Kunz, O.; Wagner, W., The GERG-2008 wide-range equation of state for natural gases and other mixtures: an expansion of GERG-2004. *J. Chem. Eng. Data* **2012,** 57, 3032-3091.
23. Seville, A. H., The heat capacity of platinum at high temperatures. *The Journal of Chemical Thermodynamics* **1975,** 7, 383-387.

24. Lemmon, E. W.; Bell, I. H.; Huber, M. L.; McLinden, M. O. *NIST Standard Reference Database 23: Reference Fluid Thermodynamic and Transport Properties-REFPROP, 10.0*; National Institute of Standards and Technology: Gaithersburg, MD; 2018.
25. Tegeler, C.; Span, R.; Wagner, W., A new equation of state for argon covering the fluid region for temperatures from the melting line to 700 K at pressures up to 1000 MPa. *J. Phys. Chem. Ref. Data* **1999,** 28, 779-850.
26. Setzmann, U.; Wagner, W., A new equation of state and tables of thermodynamic properties for methane covering the range from the melting line to 625 K at pressures up to 100 MPa. *J. Phys. Chem. Ref. Data* **1991,** 20, 1061-1155.
27. Lemmon, E. W.; McLinden, M. O.; Wagner, W., Thermodynamic properties of propane. III. A reference equation of state for temperatures from the melting line to 650 K and pressures up to 1000 MPa. *J. Chem. Eng. Data* **2009,** 54, 3141-3180.
28. Lemmon, E. W.; Jacobsen, R. T., Viscosity and thermal conductivity equations for nitrogen, oxygen, argon, and air. *Int. J. Thermophys.* **2004,** 25, 21-69.
29. Friend, D.; Ely, J.; Ingham, H., Tables for the thermophysical properties of methane. **1989**.
30. Marsh, K. N.; Perkins, R. A.; Ramires, M. L. V., Measurement and correlation of the thermal conductivity of propane from 86 K to 600 K at pressures to 70 MPa. *J. Chem. Eng. Data* **2002,** 47, 932-940.
31. Frenkel, M.; Chirico, R. D.; Diky, V.; Yan, X.; Dong, Q.; Muzny, C., ThermoData Engine (TDE): software implementation of the dynamic data evaluation concept. *J. Chem. Inf. Model.* **2005,** 45, 816-838.
32. Chichester, J. C.; Huber, M. L., *Documentation and Assessment of Transport Property Model for Mixtures Implemented in NIST REFPROP (Version 8.0)*. US Department of Commerce, Technology Administration, National Institute of Standard and Technology: 2008.
33. Huber, M. L.; Hanley, H. J. M., The corresponding-states principle: dense fluids. In *Transport Properties of Fluids: Their Correlation, Prediction and Estimation*, Millat, J.; Dymond, J. H.; Nieto de Castro, C. A., Eds. Cambridge University Press: New York, 1996; Vol. 285, p 283−295.
34. InfoChem KBC Advanced Technologies PLC *MultiFlash 6.2*, 2019.

TOC Graphic